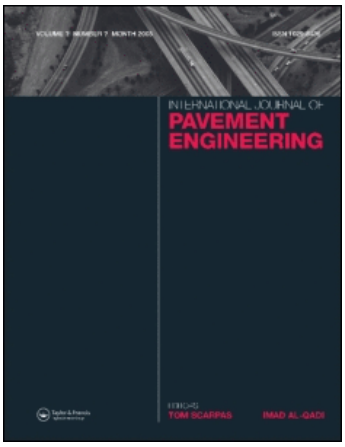

International Journal of Pavement Engineering
Publication details, including instructions for authors and subscription information:
http://www.informaworld.com/smpp/title~content=t713646742

Quantifying built-in construction gradients and early-age slab deformation caused by environmental loads in a jointed plain concrete pavement

Steven A. Wells [a]; Brian M. Phillips [a]; Julie M. Vandenbossche [a]
[a] University of Pittsburgh, Pittsburgh, PA, USA

Online Publication Date: 01 December 2006

To cite this Article Wells, Steven A., Phillips, Brian M. and Vandenbossche, Julie M.(2006)'Quantifying built-in construction gradients and early-age slab deformation caused by environmental loads in a jointed plain concrete pavement',International Journal of Pavement Engineering,7:4,275 — 289

To link to this Article: DOI: 10.1080/10298430600798929

URL: http://dx.doi.org/10.1080/10298430600798929

International Journal of Pavement Engineering, Vol. 7, No. 4, December 2006, 275–289

Quantifying built-in construction gradients and early-age slab deformation caused by environmental loads in a jointed plain concrete pavement

STEVEN A. WELLS†¶, BRIAN M. PHILLIPS†§ and JULIE M. VANDENBOSSCHE‡*

†University of Pittsburgh, 1121 Benedum Hall, Pittsburgh, PA 15261, USA
‡University of Pittsburgh, 934 Benedum Hall, Pittsburgh, PA 15261, USA

(Received 6 December 2005; revised 6 April 2006)

Construction curling and warping produces a built-in gradient, which takes place as the result of changes in temperature and moisture that occur prior to the hardening of Portland cement concrete (PCC) pavements. The slab remains flat in the presence of this gradient because the plastic concrete has not developed sufficient stiffness to generate stress or strain. The new Guide for the Design of New and Rehabilitated Pavement Structures has shown the importance of quantifying the built-in gradient. In this study, the magnitude of the built-in gradient was quantified along with the early-age response of the slab to environmental loads. It was found that the equivalent linear temperature gradient at the time of set was <0.09°C/cm (0.55°F/in.). The largest built-in curvature measured along the diagonal for the restrained and unrestrained slabs was 0.0000124 1/m (0.0000408 1/ft) and 0.0000138 1/m (0.0000454 1/ft), respectively. The increase in curvature with an increase in equivalent linear temperature gradient for the unrestrained slabs was 7% higher than the restrained slabs. The profiles also indicated that the slab edges are, at times, completely unsupported.

Keywords: Concrete; Curling; Warping; Non-linear gradients; Curvature

1. Introduction

The climatic conditions at the time of paving can greatly affect the performance of the slab. Climatic conditions are also important when characterizing the effects of curling and warping. Among other things, these conditions dictate the magnitude of the built-in construction gradient. Construction curling and warping is the result of a built-in gradient, which occurs as changes in temperature and moisture occur throughout the depth of the slab prior to hardening of the Portland cement concrete (PCC) (Yu and Khazanovich 2000). Slabs that are constructed during the daytime gain a significant amount of heat energy from solar radiation and hydration of the cement. At night, as the ambient temperature drops and both moisture and heat energy are lost near the surface of the PCC, a negative built-in temperature gradient develops. The slab remains flat even in the presence of this negative gradient because the plastic concrete has not developed sufficient stiffness to generate stress or strain. The new Guide for the Design of New and Rehabilitated Pavement Structures (2004) has shown the importance of quantifying the built-in gradient (Yu and Khazanovich 2000). Both pavement instrumentation and analytical models are being used to better characterize the effect of temperature and moisture gradients on the performance of concrete pavements (Jeong *et al.* 2001, Jeong and Zollinger 2004). The magnitude of the built-in gradient for a pavement constructed on S.R.-22 in Murrysville, Pennsylvania was quantified along with the early-age response of the slab to temperature and moisture gradients. A thorough investigation on slab response to gradients that develop within the slab throughout the first week after paving is provided below.

2. Overview of test section

The instrumented pavement in this study consists of a 30 cm (12 in.) Portland cement jointed plain concrete pavement (JPCP) constructed on top of a 10 cm (4 in.) open-graded asphalt stabilized base, a 13 cm (5 in.) dense-graded sub-base, and a 61 cm (24 in.) backfill

*Corresponding author. Tel.: 1 412 624 9879. Fax: 1 412 624 0135. Email: jmv@engr.pitt.edu
¶Tel.: + 412-624-9863. Fax: + 412-624-0135. Email: saw23@.pitt.edu.
§Tel.: + 412-624-9863. Fax: + 412-624-0135. Email: bmp6@.pitt.edu.

International Journal of Pavement Engineering
ISSN 1029-8436 print/ISSN 1477-268X online © 2006 Taylor & Francis
http://www.tandf.co.uk/journals
DOI: 10.1080/10298430600798929

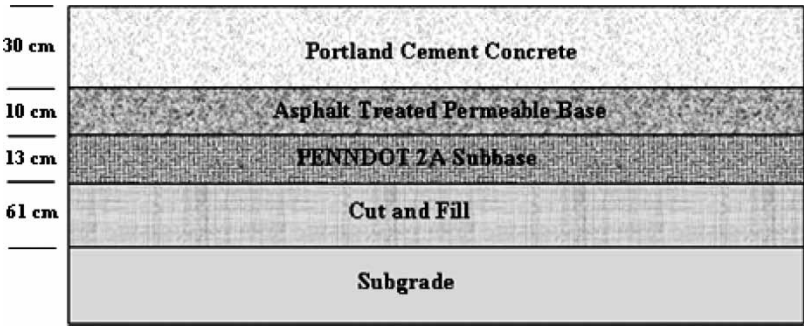

Figure 1. Design thicknesses of the pavement layers.

material, as shown in figure 1. This pavement was constructed on a section of highway on US Route 22 in Murrysville, Pennsylvania (Wells *et al.* 2005).

The new JPCP is a four-lane divided highway with 4.6 m (15 ft) transverse joints, 3.7 m (12 ft) lanes, and 0.8 m (2.6 ft) wide concrete curb-and-gutter shoulders. The pavement contained 3.8 cm (1.5 in.) diameter dowels along the transverse joints and 1.6 cm (0.625 in.) diameter tie bars spaced 3 ft on center along the centerline joint, as shown in figure 2.

Figure 3 provides an overview of the overall test section layout. The test section is located in the westbound truck lane of Route 22 and consists of seven PCC slabs. The dowel and tie bars were left out of three consecutive slabs so the effect of restraint they impose on the slab could be quantified. A transition slab separates the restrained and unrestrained slabs, as shown in figure 3. Each lane was paved independently using a single-lane slip-form paver. The passing lane was paved several weeks prior to the truck lane, which contained the instrumentation.

Figures 4 and 5 show the instrumentation layout for both the restrained and unrestrained slabs. The instrumented slabs contained Geokon 4200 vibrating wire static strain gages. In order to directly compare strain response in restrained versus unrestrained slabs, the layout of the gages was replicated for both sets of slabs, as shown in figure 4. The slabs were also instrumented with temperature and moisture sensors. Type T thermocouples were installed at various depths throughout the concrete and throughout the pavement structure to accurately quantify thermal gradients. The thermocouples were installed in the restrained slabs at midpanel and at the corner of the slab in two replicate locations. Sensirion SHT75 relative humidity and temperature sensors were also installed throughout the restrained slabs at midpanel and at the corner of the slab in two replicate locations. Procedures developed at the University of Illinois at Urbana-Champaign for the use of these sensors in concrete applications were followed (Grasley *et al.* 2003). Wind speed, temperature and relative humidity were measured in the field using an on-site weather.

3. Built-in construction curling and warping

Temperature gradients throughout the pavement structure are affected by both seasonal and daily environmental conditions. The top of the pavement is affected

Figure 2. Dowel and tie bar configuration on SR-22.

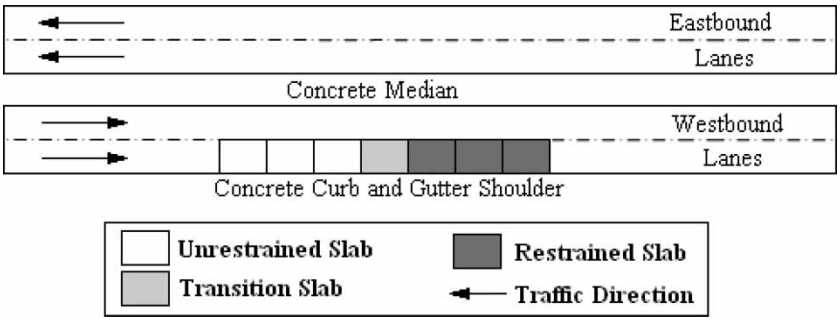

Figure 3. Layout of test section.

predominantly by daily environmental changes while the bottom varies more seasonally. Positive gradients force the edges and corners of the pavement downwards thereby increasing support in these locations and decreasing the support at the center of the slab. Corner and edge loads may result in decreased deflections under these conditions because the contact area and/or pressure between the slab and the underlying layer is increased. Negative gradients force the corners and edges of the pavement upwards and the center of the pavement downwards, thereby reducing support at the corners while increasing it at midpanel, this results in decreased midpanel deflections and increased corner and edge deflections.

The slab does not generally lie flat when a temperature/moisture gradient is not present because the concrete slab typically sets with a temperature gradient present, resulting in permanent deformation. The temperature gradient present at the time the concrete sets is referred to as the construction gradient, as discussed previously. The magnitude of the construction gradient is largely influenced by the time of the day at which the concrete is placed and by the daily fluctuations in the ambient temperature. The construction gradient is a required input for the 2002 Guide for the Design of New and Rehabilitated Pavement Structures but there currently is insufficient data available to define what this input should be with any level of confidence either locally or nationally.

The test section was paved on August 1, 2004 at approximately 7:00 am. Figure 6 shows the temperature distribution throughout the pavement and sub-layers at the time of paving, setting, and joint cracking. The estimated time of set of 10 h was based on static strain. Figure 7 shows strain versus change in temperature. The set time was defined as the time strain began to develop with changes in temperature. This was also about the same time the joints were sawed. At the time of set, there was a linear gradient of 0.2°C/cm (0.7°F/in.) at the edge and practically no gradient at midpanel. However, since the gradient is not linear, identifying the gradient as zero does not do justice to the large internal differences in temperature present at the time of set, as seen in figure 6.

The joints cracked approximately 17–19 h after paving. At this time there was a large negative gradient of about

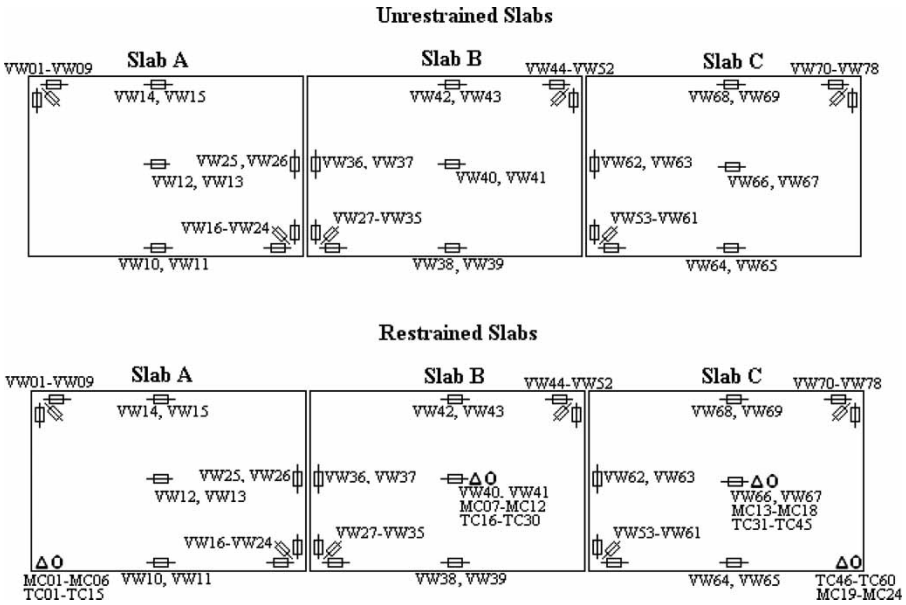

Figure 4. Instrumentation layout of test section.

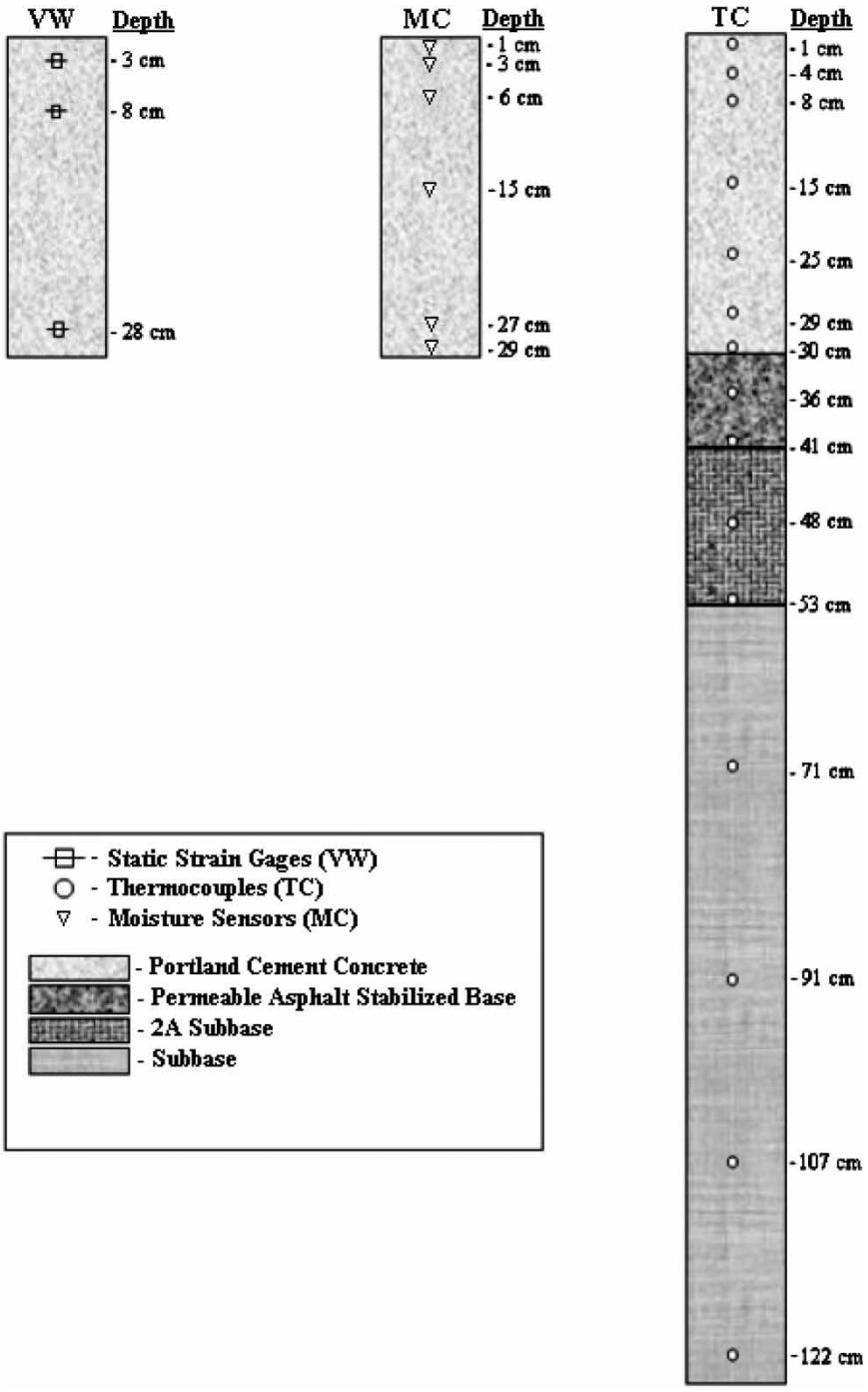

Figure 5. Instrumentation depths throughout pavement structure.

−0.2°C/cm (−1.0°F/in.), as shown in figure 8, which produced enough stress to crack the slab.

Figure 8(a),(b) show the temperature distribution at midpanel and the edge of the slab, respectively. These graphs illustrate the fact that the temperature distribution throughout the slab is not uniform so the deformation produced by the temperature gradients in the slab will not be symmetrical. The temperature generated within the slab is a function of the boundary conditions. The slab is cast along a pre-existing slab on one side (centerline edge) and the other edge (lane/shoulder edge) is exposed to ambient conditions since the curb and gutter were constructed after the lane was paved. At midpanel, the heat will be retained more than at the lane/shoulder edge where the slab is exposed to the cooler evening temperatures throughout the depth of the pavement. This is why the edge of the pavement will be approximately the same temperature throughout the depth of the slab. A depiction of the spatial distribution of temperature across the top and bottom of the slab is provided in figure 9. Temperatures shown in figure 9 were obtained from strain gage thermistors embedded 25 mm

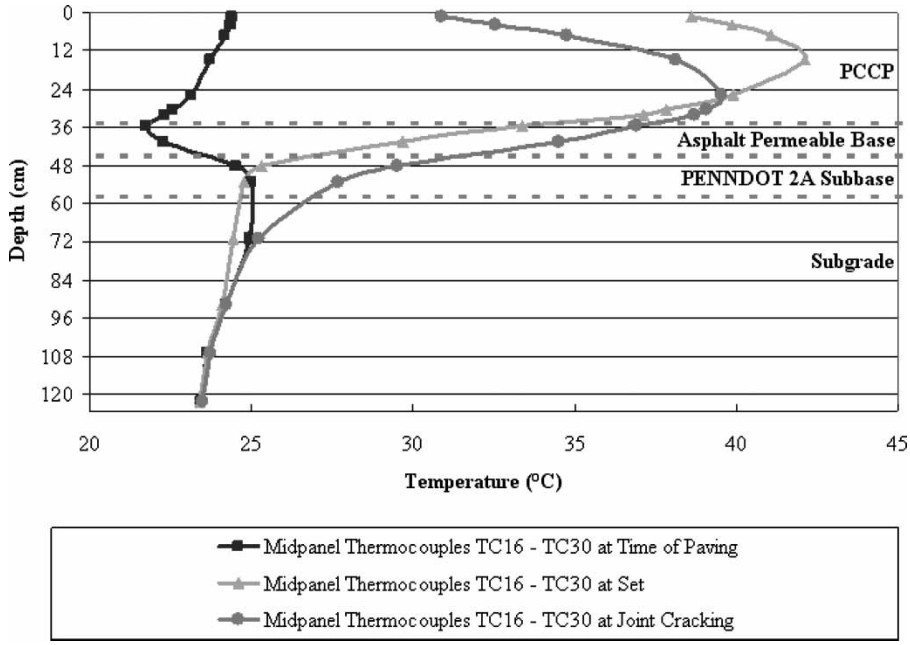

Figure 6. Temperature distribution throughout depth at midpanel.

(1 in.) from the top and 25 mm (1 in.) from the bottom of the slab at the time the joints cracked.

Figure 10 shows more clearly the difference between gradients at midpanel and at the edge. It is apparent that the midpanel is subject to more dramatic temperature swings during the day. These larger swings result in the development of larger gradients at the midpanel. As shown in figure 10, even adding on the curb and cutter does not completely negate the effect between the temperatures at the edge of the slab and at midpanel.

Figures 11 and 12 show the relative humidity throughout the depth of the slab measured at midpanel and in the corner, respectively. The curb and gutter was not tied onto the pavement at this time so the edge of the slab is exposed to the ambient climatic conditions. The relative humidity, especially near the pavement surface continues to drop after paving. There was a rain event on August 19 that produced 15 mm (0.6 in.) of precipitation, on August 20 that produced 25 mm (1 in.) of precipitation and on August 21 that produced 8 mm (0.3 in.) of precipitation. These rain events resulted in an increase in relative humidity near the pavement surface at midpanel. The relative humidity increased throughout the depth of the slab near the corner where the whole edge of the slab is exposed to the rain. The relative humidity in the concrete is around 92–94%. These are comparable to those reported by Jeong *et al.* (2001).

4. Non-linear temperature gradients

The temperature gradients described earlier are calculated simply by dividing the temperature at the top and the bottom of the pavement by the distance between them. The shortcoming of this method is that it provides a linear relationship while non-linear gradients are known to exist in the pavement. In order to account for the non-linear temperature gradients, the parameter "temperature moment" was developed by Janssen and Snyder, 2000 (Jeong *et al.* 2001). The temperature moment was developed so that a non-linear gradient can be equated to an equivalent linear gradient based on an equivalent strain condition. Figure 13 graphically summarizes the derivation of temperature moment for any given period of time within the concrete pavement. Temperature moment can be calculated using equations (1) and (2). The temperature moment can then be used to find the equivalent linear temperature gradient using equation (3) based on an equivalent strain.

$$\mathrm{TMo} = -0.25\sum_{i=1}^{n}\left[(t_i + t_{i+1})(d_i - d_{i+1}) - 2(d_1^2 - d_n^2)T_{\mathrm{wave}}\right] \tag{1}$$

TMo, temperature moment (figure 13); t_i, temperature at location$_i$; d_i, depth at location$_i$; T_{wave}, weighted average temperature (equation (2))

$$T_{\mathrm{wave}} = \sum_{i=1}^{n}\left[\frac{(0.5)(t_i + t_{i+1})(d_i - d_{i+1})}{(d_1 - d_n)}\right] \tag{2}$$

T_{wave}, weighted average temperature (equation (2))

$$\mathrm{ELG} = -\frac{12(\mathrm{TMo})}{h^3} \tag{3}$$

ELG, equivalent linear gradient; h, slab thickness.

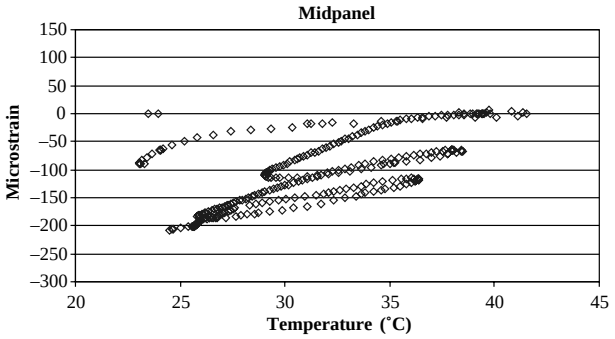

Figure 7. Strain versus temperature at midpanel for the first 72 h after

5. Surface profile measurements

In order to quantify the effect of early-age (first 72 h) effects of curling and warping on PCC pavements, surface profile measurements are taken. These profile measurements capture the shape of the slab under various temperature and moisture gradients. In order to measure the surface profiles of slabs experiencing thermal and moisture gradients, an instrument called a dipstick, manufactured by Face Construction Technologies, Inc. was utilized. The dipstick pictured in figure 14(a), is a highly sensitive device that measures difference in

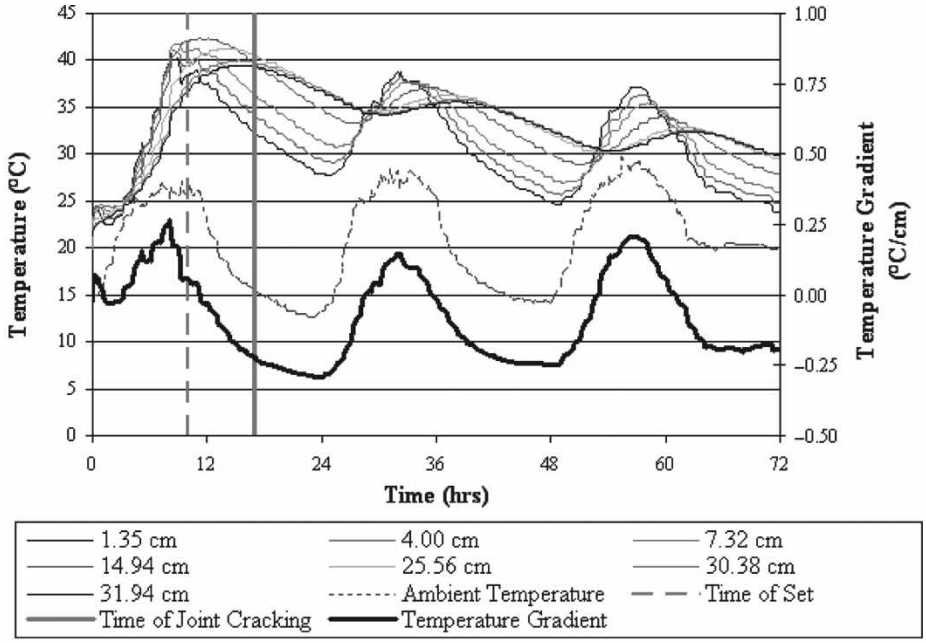

a. Midpanel

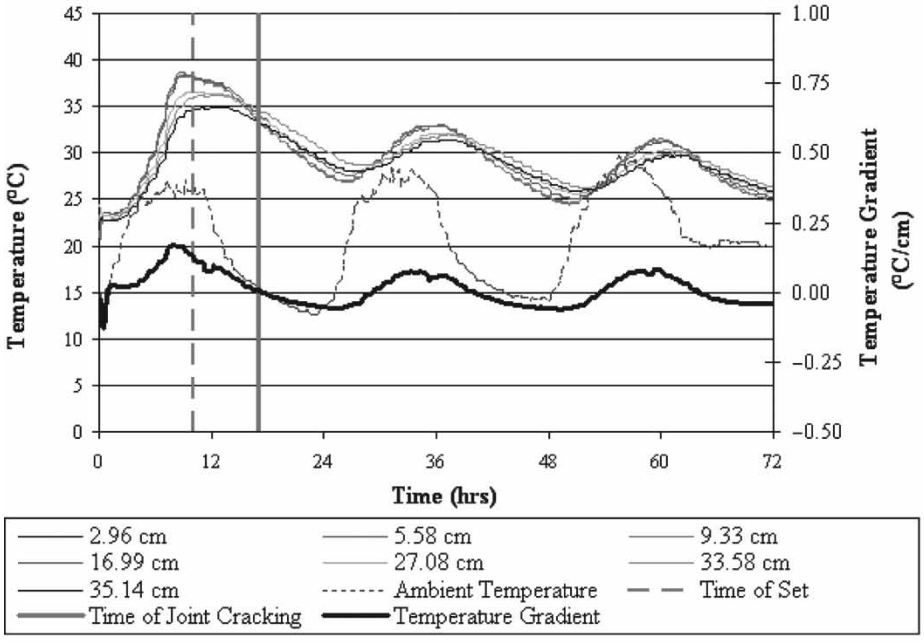

b. Edge

Figure 8. Temperature distribution and temperature moments within concrete slab and ambient temperatures.

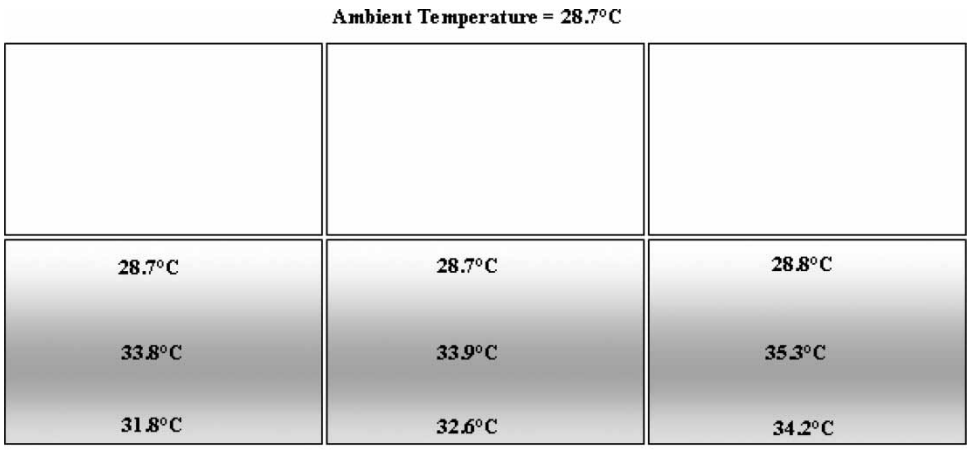

a. Top of the slab.

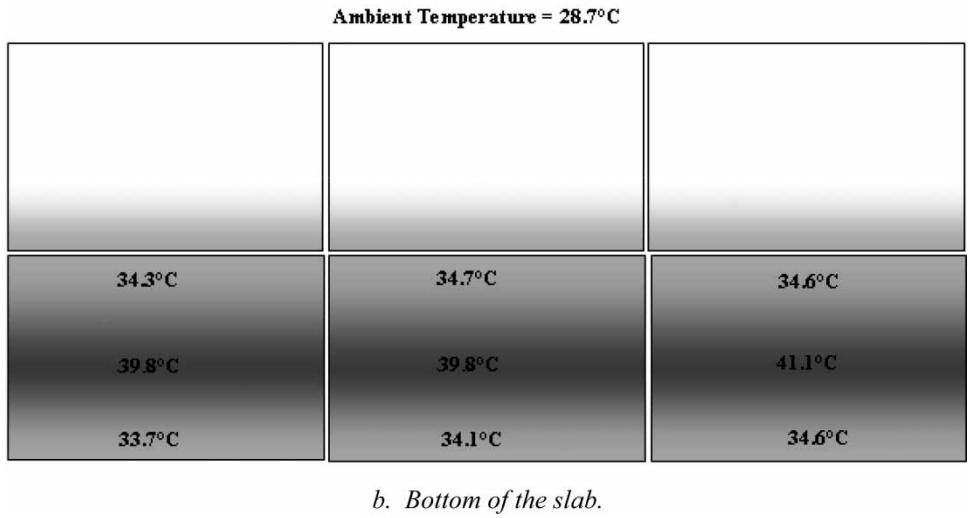

b. Bottom of the slab.

Figure 9. Representation of the spatial temperature distribution across the slab at the time of concrete cracking.

elevation between successive points along a PCC surface. When walked across a PCC slab, relative elevations of the slab profile, and hence curling and warping can be measured. Surface profiles were measured across the slab in the longitudinal, diagonal, and transverse directions, as outlined in figure 14(c).

Note the two circular objects located near the transverse joints along the shoulder in figure 14(c). These objects represent the tops of invar rods which were placed in the ground at a depth of approximately 3.7 m (12 ft). In order to further insure the consistency of this reference elevation, the upper portions of the invar rods were encased in grease-filled polyvinylchloride (PVC) tubing in order to protect the rods from the expansive stresses induced by frost exposure. The top of this rod, pictured in figure 14(b), maintains a constant elevation throughout the year and is thus used as a benchmark for all slab profile measurements. Initiating each dipstick run off from the top of the rod allows all relative elevations measured with the dipstick to be tied into actual elevations.

The dipstick was able to provide a dynamic representation of the concrete slab surface profile as daily temperature moments caused it to curl. The main focus of this analysis was to evaluate the curling response to different joint conditions, in particular between those with and without dowel and tie bars. Note that imperfections in the slab were taken into account by zeroing each profile based on the time the concrete set. The equivalent linear temperature gradient at the time of set was less than 0.09°C/cm (0.55°F/in.). All profile measurements discussed below were made prior to the placement of the curb and gutter.

Representative slab profiles measured in the transverse direction are shown in figures 15 and 16. Profiles measured along the longitudinal and diagonal were not included due to space restrictions but can be found in reference 5. The figure contains profiles measured at different times of the day for both the restrained (slabs containing dowel and tie bars) and unrestrained (slabs without dowel or tie bars) slabs. All profiles were measured within the first week after paving.

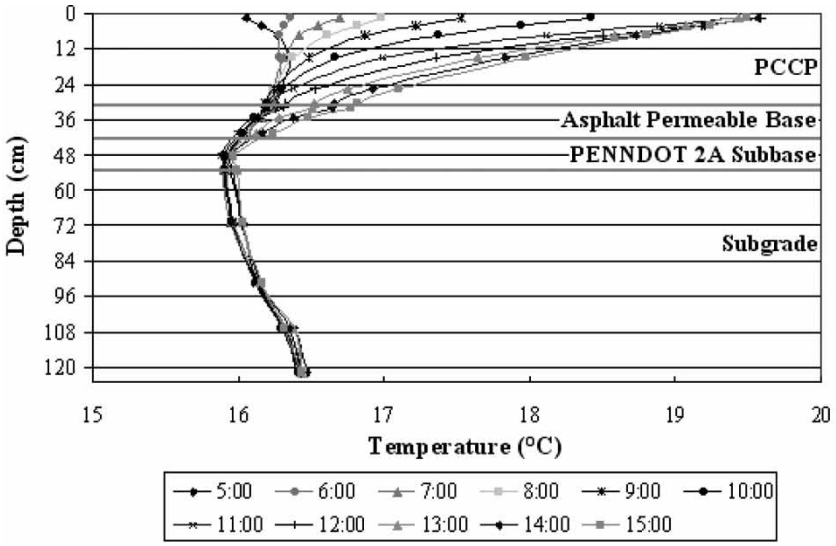

a. Midpanel

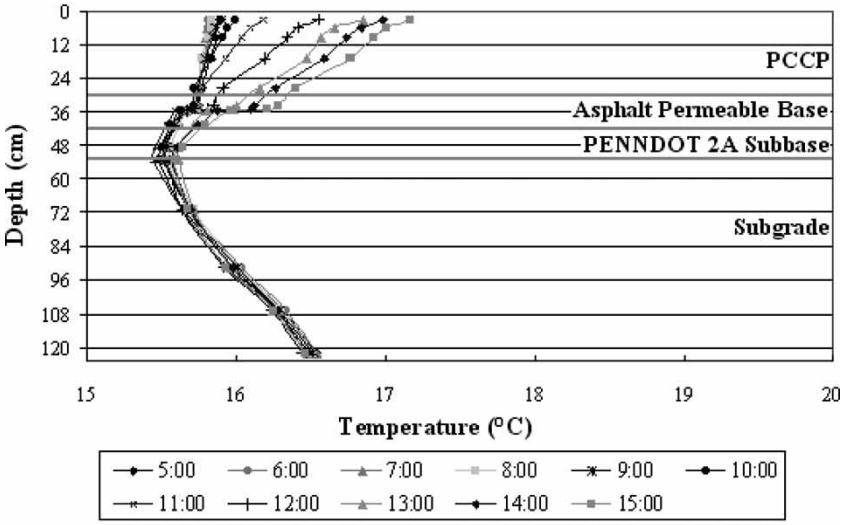

b. Edge

Figure 10. Temperature gradient in the slab during a 10 h period on October 31, 2005.

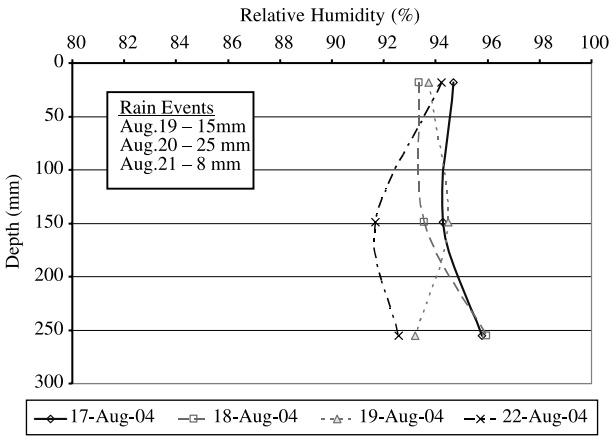

Figure 11. Moisture measurements made at midpanel.

Profiles across the diagonal lines were similar for unrestrained and restrained slabs. The longitudinal profiles showed the greatest difference between unrestrained and restrained slabs. The reason for this could draw from the fact that during the time period for which the profiles were measured, there was no curb adjacent along the longitudinal joint so the restraint conditions were the same for both cells. Since the edge of the slab was exposed to the ambient climatic conditions, temperature gradients did not develop within the slab along the edge. This could be another reason why the curvature in the longitudinal profile was small. In the transverse direction, the profiles of the unrestrained slabs exhibit slightly more movement at the edges.

As would be expected, the maximum displacement for the unrestrained slab was substantially higher than the restrained slab. The movement of the end of an unrestrained slab as a result of curling and warping can be as much as twice as high compared to the restrained slab.

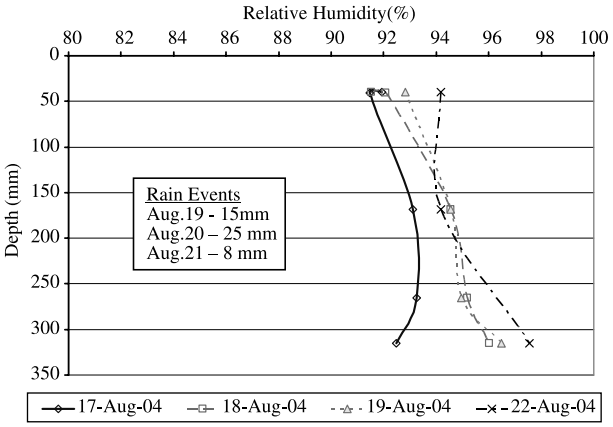

Figure 12. Moisture measurements made at the corner of the slab.

A displacement of zero or less indicates the slab is in contact with the base. A portion of the slab is always in contact with the base when looking at the diagonal but many times the edge of the slab will be completely unsupported in both the transverse and longitudinal directions. This is true for both the restrained and unrestrained slabs.

Another trend seen is that the movement of the slab as a whole is far less for the restrained slabs then the unrestrained slabs. This is indicated by the more tightly grouped profiles depicted in the displacements graphs for the restrained slabs compared to the unrestrained slabs. The restraint provided by the dowels at the transverse joint greatly reduces the curvature at the end of the slab. Part of this can also be attributed to the fact that fewer measurements were made for the restrained slabs and the gradients were not as high when the measurements were made.

6. Slab curvature before and after the joints crack

The curvature for each profile was then calculated by fitting a second order polynomial to the measured profile. The curvature of the polynomial was calculated 1 ft into the slab from the shoulder. By combining the profile data with the equivalent linear gradient derived from the midpanel thermocouples, the relationship between slab curvature and equivalent linear temperature was defined.

The response of the slab to temperature gradients before and after the joints crack is quite different, as would be expected since the effective slab length is substantially longer. Figure 17 shows the curvature calculated for profiles measured before and after the joints cracked for slab A (figure 4) in the unrestrained cell. The curvature calculated before the joints cracked (shown as solid circles) are well below the best-fit line of all of the data points. In all cases except when the equivalent linear gradient is quite high, curvature calculated before cracking will be less than curvature calculated after cracking by a factor of two.

7. Effect of midpanel temperature on slab curvature

Figures 18–23 illustrate the relationship between curvature and equivalent linear temperature gradient. The curvatures for the diagonal profiles measured for the unrestrained and restrained slabs are provided in figures 18 and 19, respectively. Curvatures calculated for the transverse and longitudinal profiles are summarized in figures 20–23, respectively. Only the curvatures calculated for the profiles measured after the slab cracked were used to generate the plots.

In this analysis, the slope of the line indicates the rate of increase in curvature with an increase in equivalent linear temperature gradient. The slopes of the restrained profiles are on average 7% less than those of the unrestrained. The maximum curvatures for the restrained slab are also substantially less than the unrestrained. This can be observed best for the diagonal profiles since in the longitudinal and transverse directions for the restrained slabs, few profiles were measured during the occurrence of high temperature gradients. The reduction in curvature for

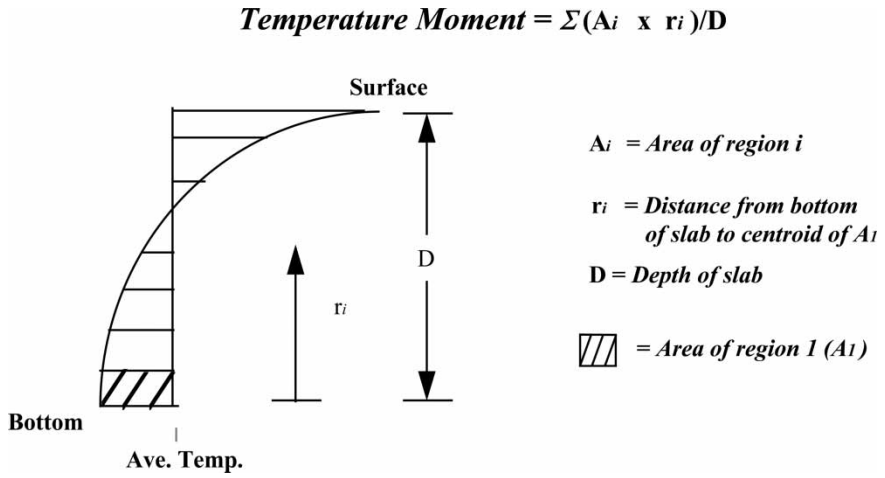

Figure 13. Graphical method for showing the temperature moment calculations (Jeong and Zollinger 2004).

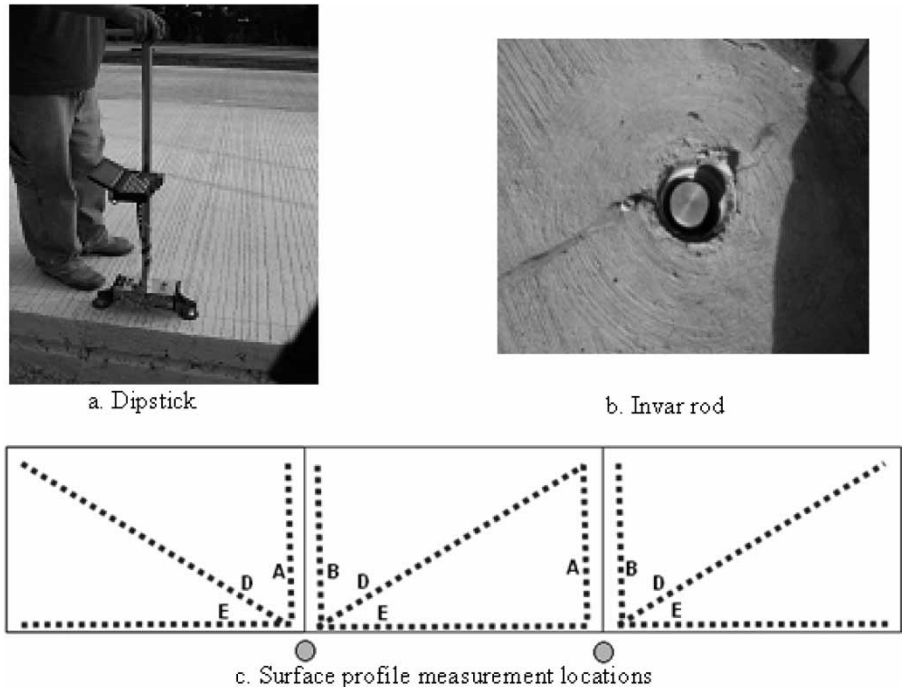

Figure 14. Surface profile measurement paths.

the restrained slab provides an indication of the stress that develops within the slab when this curvature is restrained.

Another notable aspect found for the transverse joints is that the rate in increase in curvature with increasing equivalent linear gradient (slope of the line) for restrained transverse joints seems to be more uniform than for unrestrained joints. In the restrained joints, shown in figure 23, the transverse profile A of slab A and profile B of slab B are measured on opposing sides of the joint while profile A of slab B and profile B of slab C are also measured on opposite sides of a joint. Overall the slopes seem similar, despite the lack of data for higher temperature moments. Looking at the transverse profiles measured on opposite sides of the unrestrained joints, profiles measured along the joint between slabs B and C exhibit a slightly larger slope than the profiles measured along the transverse joint between slabs A and B. The difference between the curvature along the two joints is the result of the joint cracking pattern. The joint between slabs A and B cracked first and was a wider crack than the crack at the joint between slabs B and C. The larger crack opening results in less restraint and therefore a greater amount of curvature will develop for equivalent gradients.

The *y*-intercept is dependent on the time the slab set and the resulting curvature set into the slab (built in curvature). In other words, it is the curvature present when a temperature gradient is not present in the slab. This will be a function of the time each slab was paved, the

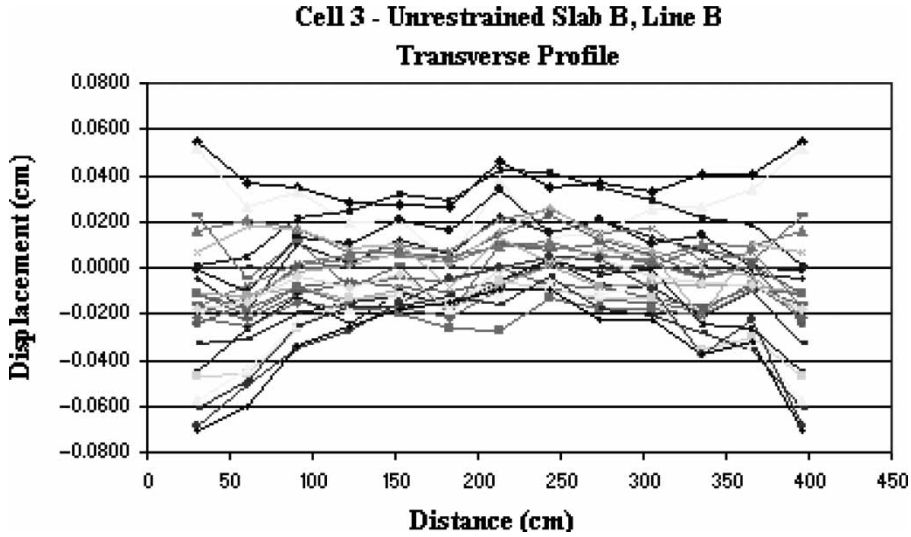

Figure 15. Transverse profiles for an unrestrained slab.

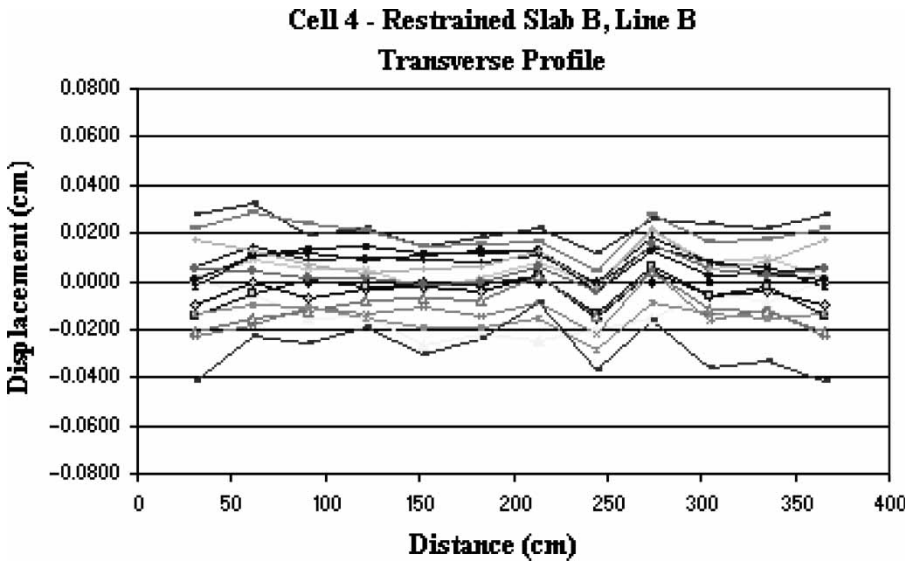

Figure 16. Transverse profiles for a restrained slab.

temperature gradients that developed throughout the day and the restraint conditions. The largest built in curvature measured along the diagonal for the restrained and unrestrained slabs was 0.0000124 1/m (0.0000408 1/ft) and 0.0000138 1/m (0.0000454 1/ft), respectively. The average built in curvature for the restrained slabs was 0.0000103 1/m (0.0000337 1/ft) with a standard deviation of 0.00000263 1/m (0.00000864 1/ft). The average built in curvature for the unrestrained slabs was 0.0000123 1/m (0.0000405 1/ft) with a standard deviation of 0.00000142 1/m (0.00000465 1/ft).

7.1 Effect of edge slab temperature on slab curvature

Before beginning the analysis, the midpanel and edge slab temperatures were evaluated to determine which was most influential on slab response (curvature). The temperature gradients in the preceding figures were all based on the midpanel thermocouples. Since the longitudinal profile was measured along the edge of the slab, the relationship between equivalent linear temperature gradients calculated using the thermocouples along the edge of the slab was evaluated. These figures were not included here due to the space limitations. It was apparent by the substantial reduction in the coefficient of determination, the relationship between equivalent linear temperature gradients calculated using the thermocouples at the edge and curvature is not nearly as strong as when using the thermocouples at midpanel to calculate equivalent linear temperature gradients. This reveals that the response of the slab along the longitudinal edge is controlled by the

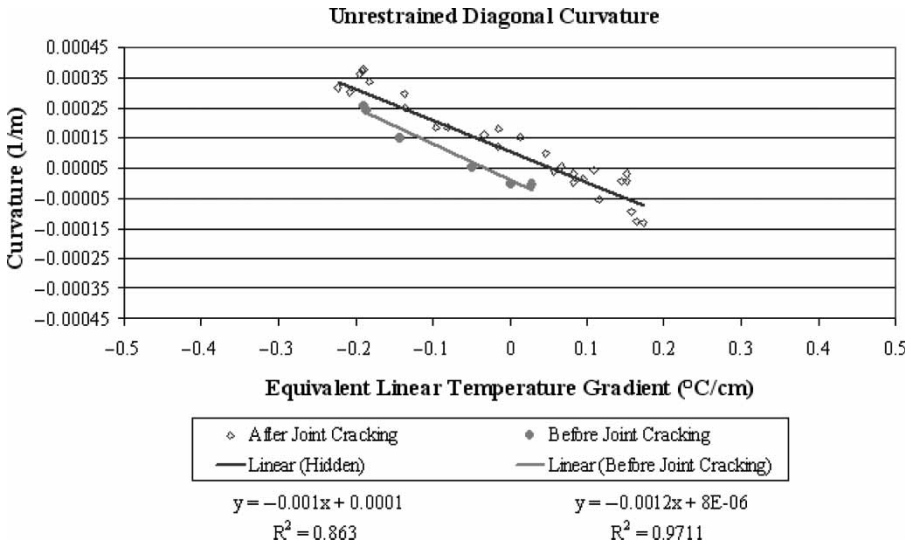

Figure 17. Illustration of the relationship between equivalent linear temperature gradient and curvature before and after joint cracking for the diagonal profiles of the unrestrained cell.

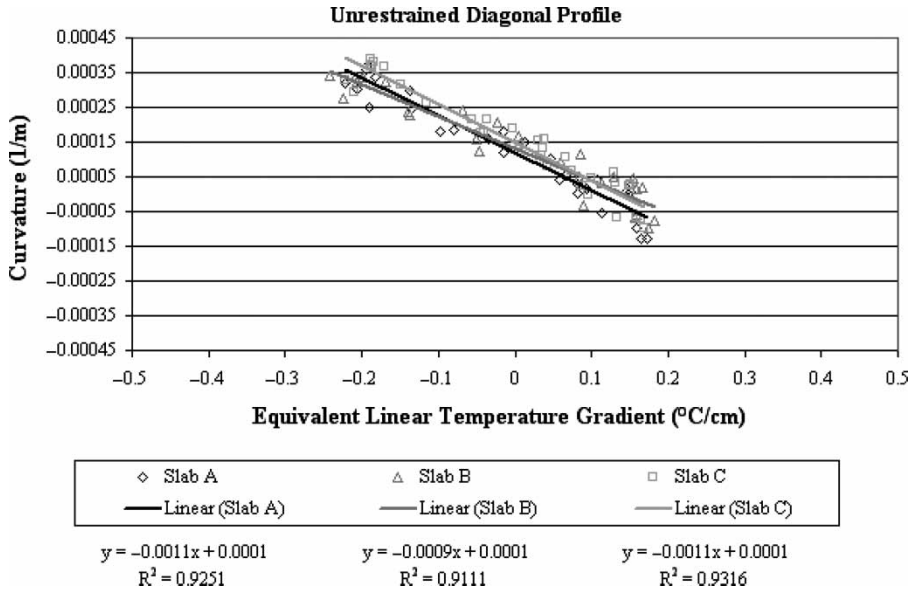

Figure 18. Equivalent linear temperature gradient versus curvature for diagonal profiles at unrestrained slabs.

temperature of the slab at midpanel more so than the edge. The restrained cell seems to correlate to the equivalent linear temperature gradients along the edge of the slab even less than the unrestrained.

8. Conclusions

The surface profiles give insight into the response of the pavement to early-environmental loads, in particular temperature. The equivalent linear temperature gradient at the time of set was <0.09°C/cm (0.55°F/in.). Since the concrete set at a time when little gradient was present, a full range of curvatures both positive and negative can be seen in the profiles. The largest built in curvature measured along the diagonal for the restrained and unrestrained slabs was 0.0000124 1/m (0.0000408 1/ft) and 0.0000138 1/m (0.0000454 1/ft), respectively. The average built in curvature for the restrained slabs was 0.0000103 1/m (0.0000337 1/ft) with a standard deviation of 0.00000263 1/m (0.00000864 1/ft). The average built in curvature for the unrestrained slabs was 0.0000123 1/m (0.0000405 1/ft) with a standard deviation of 0.00000142 1/m (0.00000465 1/ft).

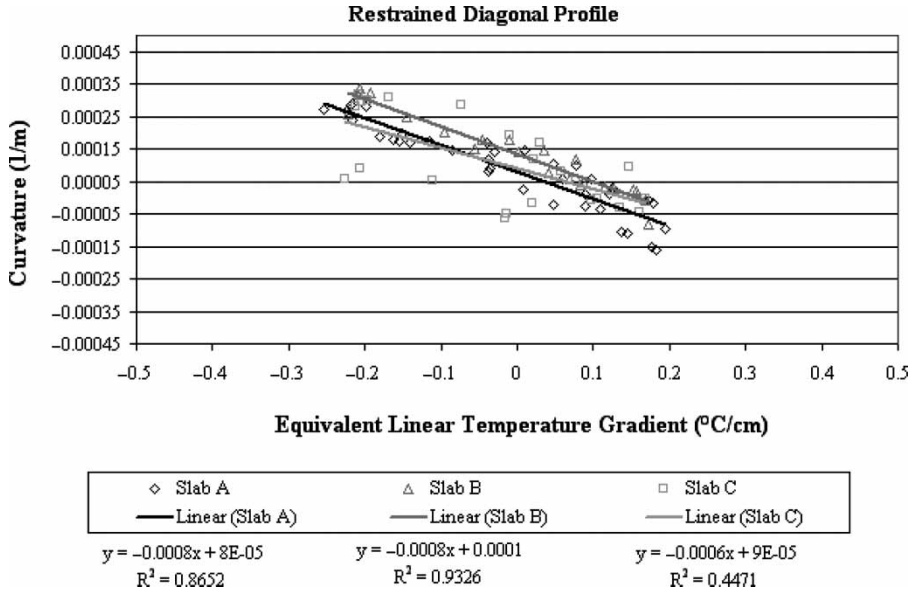

Figure 19. Equivalent linear temperature gradient versus curvature for diagonal profiles at restrained slabs.

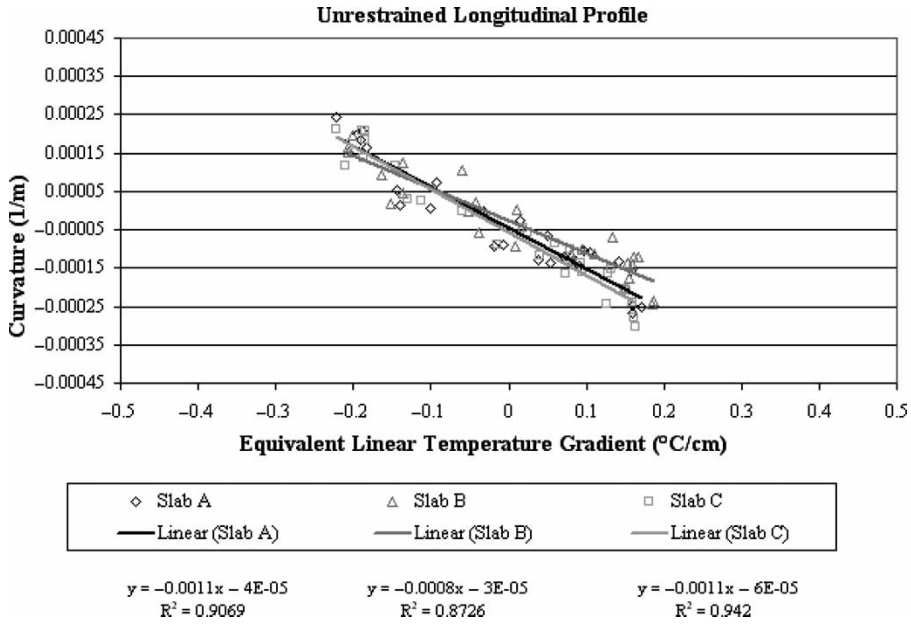

Figure 20. Equivalent linear temperature gradient versus curvature for longitudinal profiles at unrestrained slabs.

The unrestrained slabs curled more dramatically with a much larger maximum displacement than the restrained slabs. The increase in curvature with increase in temperature moment was 7% higher for the unrestrained slabs compared to the restrained slabs. The restrained slab profiles are also grouped much more closely together, indicating that the slabs moved much less along the entire length of the profile. In the longitudinal and transverse directions for both restrained and unrestrained slabs, the profiles indicated that the edges sometimes become completely unsupported.

Taking into account the curvature of the slabs, it was observed that the slabs respond differently to temperature gradients before and after setting. Looking at the difference between slab restraints, the unrestrained slabs curled much more under the same gradients than the restrained slabs. Along the transverse joint for the doweled slabs, the relationship between curvature and temperature moment was very similar. Also, the slabs exhibited greater curvature at joints with wider cracks.

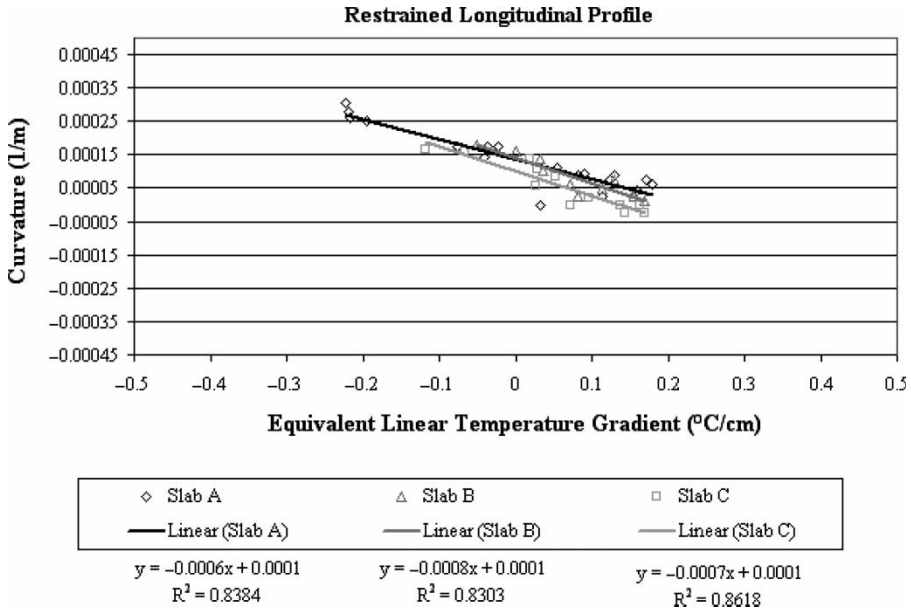

Figure 21. Equivalent linear temperature gradient versus curvature for longitudinal profiles at restrained slabs.

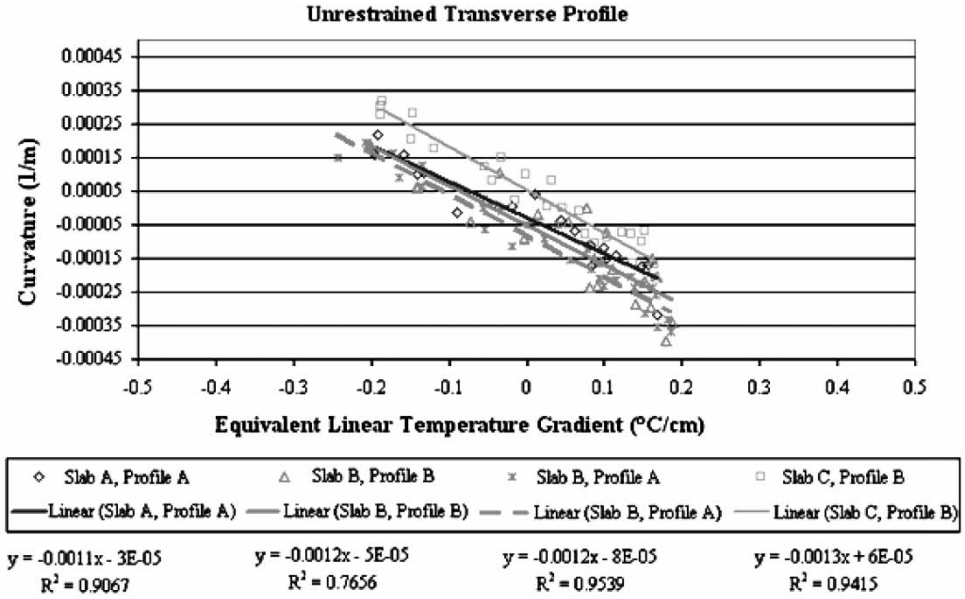

Figure 22. Equivalent linear temperature gradient versus curvature for transverse profiles at unrestrained slabs.

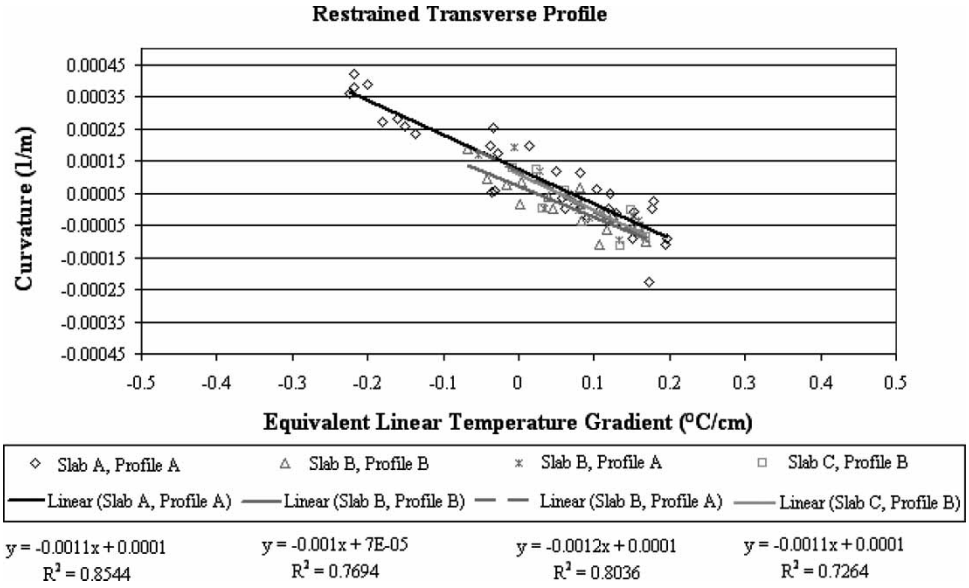

Figure 23. Equivalent linear temperature gradient versus curvature for transverse profiles at restrained slabs.

Acknowledgements

The authors would like to thank the Pennsylvania Department of Transportation (PENNDOT) and the Federal Highway Administration (FHWA) for their financial and technical support. In addition the authors would like to thank all the graduate and undergraduate students who assisted in the completion of this project.

References

Choubane, B. and Tia, M., Nonlinear temperature gradient effect on maximum warping stresses in rigid pavements. *Transportation Research Record 1370*, pp. 65–71, 1992 (Washington, DC).

Grasley, Z.C., Lange, D.A. and D'Ambrosia, M.D., Internal relative humidity and drying stress gradients in concrete. *Proceedings of Engineering Conferences International, Advances in Cement and Concrete IX*, Copper Mountain, CO, 2003.

Guide for Mechanistic-Empirical Design of New and Rehabilitated Pavement Structures—Final Report, National Cooperative Highway Research Program 1-37A, Transportation Research Board, National Research Council, March 2004.

Hveem, F.N., Slab warping affects pavement joint performance. *Journal of the American Concrete Institute*, 1951, **22**(10) Proceedings V. 47, June.

Janssen, D., Moisture in Portland cement concrete. *Transportation Research Record 1121*, 1987, Washington, DC.

Janssen, D.J. and Snyder, M.B., The temperature-moment concept for evaluating pavement temperature data. Technical note. *Journal of Infrastructure Engineering*, 2000, **6**(2), American Society of Civil Engineers. Reston, VA, June 2000, pp. 81–83.

Jeong, J.H. and Zollinger, D.G., Early-age curling and warping behavior: insights from a fully instrumented test-slab system. *Journal of the*

Transportation Research Board 1896, Transportation Research Record, Washington, DC 2004, 66–74.

Jeong, J.H., Wang, L. and Zollinger, D.G., A temperature and moisture module for hydrating Portland cement concrete pavements. *7th International Conference on Concrete Pavements*, Orlando, FL, September pp. 9–22, 2001.

Poblete, M., Salsilli, R., Valenzuela, R., Bull, A. and Spratz, P., Field evaluation of thermal deformations in undoweled PCC pavement slabs. *Transportation Research Record No. 1207*, 1988, Washington, DC.

Reddy, A.S., Leonards, G.A. and Harr, M.E., Warping stresses and deflections in concrete pavements: Part III. *Highway Research Record No. 44*, 1963, Washington, DC.

Sheehan, M.J., Field evaluation of concrete pavement curling and warping responses, Masters of Science Dissertation, Department of Civil and Environmental Engineering, University of Minnesota, Minneapolis, MN, 1999.

Vandenbossche, J.M. and Snyder, M.B., Comparison between measured slab profiles of curled pavements and profiles generated using the finite element method. *8th International Conference on Concrete Pavements*, Denver, CO, August pp. 1155–1172, 2005.

Wells, S.A., Phillips, B.M. and Vandenbossche, J.M., S.R.-22 smart pavement phase I: early-age material properties and pavement response characteristics for jointed plain concrete pavements, phase I final report, submitted to the Pennsylvania Department of Transportation and the Federal Highway Administration, June 2005.

Wiseman, J.F., Harr, M.E. and Leonards, G.A., Warping stresses in concrete pavements: part II. *Highway Research Board Proceedings*, **39**, 1960 (Highway Research Board: Washington, DC).

Yu, H.T. and Khazanovich, L., Effects of constructions curling on concrete pavement behavior. *7th International Conference on Concrete Pavements*, Orlando, FL, September pp. 55–67, 2001.